Preprints of the 21st IFAC World Congress (Virtual)
Berlin, Germany, July 12-17, 2020

Efficient Temperature Profile Estimation for Silicon Wafers based on Subspace Observers ⋆

Markus Tranninger * **Richard Seeber** ** **Martin Steinberger** *
Martin Horn *,**

* *Institute of Automation and Control, Graz University of Technology, 8010 Graz, Austria. (e-mail: markus.tranninger@tugraz.at)*
** *Christian Doppler Laboratory for Model Based Control of Complex Test Bed Systems, Institute of Automation and Control, Graz University of Technology, Graz, Austria.*

Abstract: This work proposes a computationally efficient observation algorithm for the surface temperature profile of heated silicon wafers. The observer exploits the fact that only a few modes of the original large-order model are unstable or slowly converging. In this case, it suffices to modify only these modes by the observer's output feedback gain. Compared to classical observation techniques, the proposed method allows to compute the feedback gain for a state space of lower dimension, which reduces computational complexity. A comparison of the approach with the extended Kalman-Bucy filter using experimental data shows its appealing performance.

Keywords: Subspace Observer Design, Lyapunov Exponents, Nonlinear Systems, Extended Kalman-Bucy Filter, Linear Time Varying Systems, Reduced Riccati Equation, Wafer Temperature Estimation, Rapid Thermal Processing

1. INTRODUCTION

State estimation is required in a variety of applications in process control and monitoring. Especially for model-based process control, observers are an essential tool, as usually the available measurements are limited, see Ali et al. (2015). The estimator (usually called filter in a stochastic or observer in a deterministic setting) is usually implemented on programmable logic controllers (PLCs) with limited computational power and strict memory constraints. Frequently, models in the process industry are obtained by discretizing partial differential equations in space. This discretization results in a set of ordinary differential equations (ODEs) with a large model order. This makes it challenging to realize standard observer concepts like the (extended) Kalman filter for these problems, because the computational effort to solve the filter Riccati equation may be excessively large or even not feasible due to processor and memory constraints of the available PLCs as pointed out in Ali et al. (2015) and Kleindienst et al. (2019).

The specific problem considered in this contribution is the temperature profile estimation of silicon wafers heated by light emitting diodes (LEDs). Various processes in the semiconductor industry, like thermal oxidation or chemical vapor deposition require the wafer to be kept at a specific temperature. Hence, the wafer's temperature profile is to be controlled in these so-called rapid thermal processing (RTP) applications. The surface temperature is usually measured only at specific points using pyrometers. This makes it necessary to estimate the temperature profile over the entire wafer surface in order to apply model-based control techniques, as proposed, e.g., in Kleindienst et al. (2018, 2019).

Kleindienst et al. (2018) presents a model for the heat transport in a rotating silicon wafer. The wafer is heated via a heating plate equipped with high power LEDs. The model is based on the heat equation and takes into account significant effects like the light absorption of the wafer and cooling effects caused by radiation. The distributed parameter model is discretized in space resulting in a set of (nonlinear) ordinary differential equations. An extended Kalman filter is proposed for the state estimation problem. For this approach, the computational effort is significant and powerful PLCs are required due to the large model order, see Kleindienst et al. (2019). Hence, as an alternative, a so-called late lumping approach is presented, which results in a computationally efficient observer. However, no insight on the influence of the observer gain on the stability or performance of the observer is obtained. Therefore, the gain has to be chosen empirically, which may be a challenging task in various situations.

In the present work, a subspace observer recently presented in Tranninger et al. (2020) is adopted for the temperature profile estimation problem. The proposed

⋆ The financial support by the Christian Doppler Research Association, the Austrian Federal Ministry for Digital and Economic Affairs and the National Foundation for Research, Technology and Development is gratefully acknowledged. This work was partially supported by the Graz University of Technology LEAD project "Dependable Internet of Things in Adverse Environments".

procedure is based on the idea that physically motivated high order models often possess only a few unstable or slowly converging modes. To reduce the computational complexity of the resulting observer, only these modes are modified in the observer error dynamics. This allows to solve the corresponding filter Riccati equation on a reduced-order state space. In Tranninger et al. (2020), the subspace observer is derived for a linear time-varying system. Inspired by the extended Kalman-Bucy filter, the idea is applied here to the nonlinear model developed in Kleindienst et al. (2018) by linearization along the estimated state trajectory.

It is shown that it is possible to design a computationally efficient observer with a systematically designed feedback gain obtained via a reduced order Riccati differential equation. For the problem under consideration, experimental results show that it suffices to numerically solve a scalar Riccati differential equation for a satisfying observer performance. The proposed observer algorithm is compared to a deterministic interpretation of the extended Kalman-Bucy filter and shows a comparable estimation performance at a significantly reduced computational cost.

Notation: Matrices are printed in bold capital letters whereas column vectors are bold face lower case letters. The vector $\mathbf{q}_i$ denotes the i-th column of the Matrix $\mathbf{Q}$ whose entries are denoted by q_{ij}. The time derivative $\frac{\mathrm{d}\mathbf{x}(t)}{\mathrm{d}t}$ is represented by $\dot{\mathbf{x}}(t)$ and in some cases the time dependency is omitted for the sake of better readability. The 2-norm of a vector or the corresponding induced matrix norm is denoted by $\|\cdot\|$.

2. SEMICONDUCTOR PROCESS

This section describes the considered semiconductor process together with the mathematical model derived in Kleindienst et al. (2018). The ultimate control goal is to ensure a uniform temperature profile of the wafer's surface following a desired temperature. This is required, e.g., for activating dopant or repairing damage of the wafer after ion implantations. Another application could be the treatment of the wafer surface with reactive gases to, e.g., remove hard-baked photoresist with the aid of ozone gas.

2.1 Plant Description

A silicon wafer is mounted on a chuck and rotates in the process chamber. A static heating plate equipped with high power LEDs is mounted below the rotating chuck. The LEDs emit light with a wavelength of approximately 450 nm which is absorbed by the wafer. The LEDs are grouped into four heating zones. All LEDs of one group are controlled simultaneously with a desired electrical power.

The measurement of the surface temperature is a challenging task. Infrared cameras would be desirable but cannot be used, because on one hand the silicon wafer is transparent in this wavelength range and on the other hand it is not possible to mount cameras in the process chamber due to highly reactive gases. Therefore, pyrometers are used in the present setup to measure the temperature at specific points. Four pyrometers are available to measure the temperatures in the four heating zones, see Fig. 1.

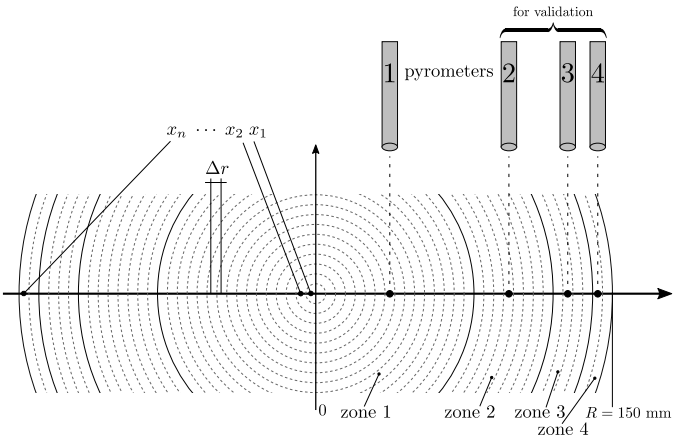

Fig. 1. Radial symmetric spatial discretization of the wafer together with the four available heating zones.

One of these is used for the state estimation, the others for validation.

2.2 Mathematical Model

The basis of the process model is the heat transfer equation for rotationally symmetric problems. This one dimensional partial differential equation is then spatially discretized with $n = 30$ grid points into concentric rings, see Fig. 1. The resulting nonlinear model is given by

$$\frac{\mathrm{d}\mathbf{x}}{\mathrm{d}t} = \mathbf{f}(\mathbf{x},\mathbf{u}) = \underbrace{\mathbf{A}_1(\mathbf{x})\mathbf{x}}_{①} - \underbrace{\varepsilon\mathbf{A}_2(\mathbf{x})\begin{bmatrix} x_1^4 \\ x_2^4 \\ \vdots \\ x_n^4 \end{bmatrix}}_{②} + \underbrace{\mathbf{B}(\mathbf{x})\mathbf{u}}_{③}. \quad (1)$$

State x_i represents the temperature in the center of the i-th ring. The first part ① of the model is related to the lossless heat equation. The heat losses through radiation are described by ②, where ε is the total emissivity, which strongly depends on the wafer type. The heat input through light absorption is described by ③. The input $\mathbf{u} \in \mathbb{R}^4$ is the electrical power supplied to the LED groups in the four heating zones. Details on the derivation on the model and the specific structure and properties of $\mathbf{A}_1(\mathbf{x})$, $\mathbf{A}_2(\mathbf{x})$ and $\mathbf{B}(\mathbf{x})$ can be found in Kleindienst et al. (2018).

In the productive setup, only one pyrometer is available to measure the temperature in zone 1. Hence, for observer design purposes the model possesses a scalar output

$$y = x_p = \mathbf{C}\mathbf{x} \quad (2)$$

with $\mathbf{C} = \mathbf{e}_p^\mathsf{T}$ and $\mathbf{e}_p$ as the unit vector corresponding to the position of pyrometer 1. The other pyrometers present in the laboratory setup are used for validation purposes.

The total emissivity ε is a characteristic quantity for a specific wafer type and in particular depends on its dopant level and coating. The parameter varies from approximately 0.2 for a "bare silicon" wafer to 0.9 for a "highly doped" wafer. In some cases, the type of the processed wafer is not known and hence it is required to estimate the total emissivity ε together with the temperature profile. In order to account for this, the state vector is extended according to $\tilde{\mathbf{x}}^\mathsf{T} = \begin{bmatrix}\mathbf{x}^\mathsf{T} & \varepsilon\end{bmatrix}$ and a new model

$$\frac{\mathrm{d}\tilde{\mathbf{x}}}{\mathrm{d}t} = \tilde{\mathbf{f}}(\tilde{\mathbf{x}}, \mathbf{u}) = \begin{bmatrix} \mathbf{A}_1(\mathbf{x})\mathbf{x} - \varepsilon \mathbf{A}_2(\mathbf{x}) \begin{bmatrix} x_1^4 \\ x_2^4 \\ \vdots \\ x_n^4 \end{bmatrix} + \mathbf{B}(\mathbf{x})\mathbf{u} \\ 0 \end{bmatrix} \quad (3)$$

$$y = [\mathbf{C}\ 0]\,\tilde{\mathbf{x}}$$

is obtained where ε is modeled as an unknown constant.

3. LYAPUNOV EXPONENTS AND THE CORRESPONDING SUBSPACES

This section recalls basic results on the stability properties of the linear time varying (LTV) systems that are required for the design of the proposed observer. The time varying system is obtained by linearizing a nonlinear system based on the ideas of the extended Kalman-Bucy filter, see Simon (2006). The system

$$\dot{\mathbf{x}}(t) = \mathbf{A}(t)\mathbf{x}(t) + \bar{\mathbf{f}}(t, \mathbf{x}),\ \mathbf{x}(t) \in \mathbb{R}^n \quad (4)$$

considered on the half line, i.e. $t \in \mathbb{J} = [0, \infty)$ with the coefficients of the matrix $\mathbf{A}(t)$ continuous and uniformly bounded and $\bar{\mathbf{f}}(t, \mathbf{x})$ as a perturbation. Such systems typically occur when linearizing a nonlinear system around a given trajectory. Stability of (4) is strongly related to the stability properties of the unperturbed system

$$\dot{\mathbf{x}}(t) = \mathbf{A}(t)\mathbf{x}(t), \quad (5)$$

which, in a first step, will therefore be investigated in the following. The unique solution of (5) is given by

$$\mathbf{x}(t) = \mathbf{\Phi}(t, t_0)\mathbf{x}_0,\ t, t_0 \in \mathbb{J} \quad (6)$$

with $\mathbf{\Phi}(\cdot, \cdot)$ as the state transition matrix and $\mathbf{x}_0 = \mathbf{x}(t_0)$ as the initial state. The state transition matrix can be obtained by any nonsingular solution of the fundamental matrix differential equation

$$\dot{\mathbf{X}}(t) = \mathbf{A}(t)\mathbf{X}(t),\ \mathbf{X}(0) = \mathbf{X}_0 \in \mathbb{R}^{n \times n} \quad (7)$$

according to

$$\mathbf{\Phi}(t, s) = \mathbf{X}(t)\mathbf{X}^{-1}(s),\ t, s \in \mathbb{J}. \quad (8)$$

The stability notions used in this work are now briefly recalled.

Definition 1. (Tranninger et al. (2020)). System (5) is *exponentially stable* if and only if there exist constants K, $\mu > 0$ such that for all $t \geq 0$ it holds that

$$\|\mathbf{\Phi}(t, 0)\| \leq K e^{-\mu t}; \quad (9)$$

It is *uniformly exponentially stable* if and only if there exist constants K, $\mu > 0$ such that for all $t_0 \in \mathbb{J}$ and all $t \geq t_0$ the inequality

$$\|\mathbf{\Phi}(t, t_0)\| \leq K e^{-\mu(t - t_0)} \quad (10)$$

holds.

Exponential stability can be studied using the functional

$$\chi^s(\mathbf{x}(\cdot)) = \limsup_{t \to \infty} \frac{1}{t} \ln \|\mathbf{x}(t)\|, \quad (11)$$

which measures the asymptotic rate of exponential growth of a function $\mathbf{x}(t)$. For $\mathbf{x}(t) = \mathbf{X}(t)\mathbf{e}_i$ with a fundamental matrix solution $\mathbf{X}(t)$ and the i-th standard basis vector, this functional attains the values λ_i, $i = 1, \ldots, n$. The sum $\sum_{i=1}^n \lambda_i$ is minimized over all fundamental matrix solutions $\mathbf{X}(t)$. The values λ_i obtained in this way are the so-called (upper) Lyapunov exponents $\lambda_i^s = \lambda_i$, see Dieci and Van Vleck (2007). It can be assumed without loss of generality that these exponents are ordered according to $\lambda_1^s \geq \lambda_2^s \geq \cdots \geq \lambda_n^s$ and the corresponding $\mathbf{X}(0)$ is then called an ordered normal Lyapunov basis. For simplicity, it is assumed that the Lyapunov exponents are distinct. Let the sets $\mathcal{V}_j$ be defined as

$$\mathcal{V}_j = \left\{\mathbf{x}_0 \in \mathbb{R}^n : \chi^s(\mathbf{\Phi}(\cdot, 0)\mathbf{x}_0) \leq \lambda_j^s\right\} \quad (12)$$

for $j = 1, \ldots, n$. It is shown in (Barreira and Pesin, 2002, p. 10) that these $\mathcal{V}_j$ are subspaces of $\mathbb{R}^n$ such that $\{0\} =: \mathcal{V}_{n+1} \subsetneq \mathcal{V}_n \subsetneq \ldots \subsetneq \mathcal{V}_2 \subsetneq \mathcal{V}_1 = \mathbb{R}^n$ with $n_j = \dim \mathcal{V}_j = \dim \mathcal{V}_{j+1} + 1$. One obtains $\chi(\mathbf{\Phi}(t, 0)\mathbf{x}_0) = \lambda_j^s$ if and only if $x_0 \in \mathcal{V}_j \backslash \mathcal{V}_{j+1}$. For an ordered normal Lyapunov basis $\mathbf{X}(0) = [\mathbf{x}_{1,0}\ \cdots\ \mathbf{x}_{n,0}]$ and distinct exponents it holds that $\mathcal{V}_i = \mathrm{span}[\mathbf{x}_{i,0}, \ldots, \mathbf{x}_{n,0}]$ and moreover $\chi^s(\mathbf{\Phi}(t, 0)\mathbf{x}_{i,0}) = \lambda_i^s$, and hence every so-called Lyapunov vector $\mathbf{x}_{i,0}$ corresponds to a specific Lyapunov exponent. It should be noted that for a constant dynamic matrix $\mathbf{A}(t) = \mathbf{A}$, the Lyapunov exponents correspond to the real parts of the eigenvalues of $\mathbf{A}$. A more detailed introduction into the theory of Lyapunov exponents including exponents with multiplicity larger than one can be found in Barreira and Pesin (2002) or as a summary in Dieci and Van Vleck (2007) and Tranninger et al. (2020).

According to Lyapunov's stability theory (Barreira and Pesin, 2002, p. 9), system (5) is (non-uniformly) exponentially stable if and only if all Lyapunov exponents are negative, i.e. $\lambda_1^s < 0$; in particular, (9) then holds for any $\mu < -\lambda_1$. Exponential stability based on negative Lyapunov exponents is not robust under small perturbations, see Barreira and Pesin (2002). However, assuming the additional property of forward regularity, which is defined later, exponential stability of (5) is preserved for (4) in the presence of sufficiently small perturbations fulfilling the conditions $\bar{\mathbf{f}}(t, \mathbf{0}) = \mathbf{0}$ and

$$\|\bar{\mathbf{f}}(t, \mathbf{x}) - \bar{\mathbf{f}}(t, \mathbf{v})\| \leq \alpha \|\mathbf{x} - \mathbf{v}\| (\|\mathbf{x}\| + \|\mathbf{v}\|)^{q-1} \quad (13)$$

for some $\alpha > 0$ and $q > 1$, see [1] (Barreira and Pesin, 2002, Theorem 1.4.3). Forward regularity is also desirable for the numerical approximation of the exponents, which will be discussed in the following.

An important tool for the numerical approximation of the Lyapunov exponents and the corresponding directions determined by Lyapunov vectors is the QR-decomposition of the fundamental matrix solution $\mathbf{X}(t) = \mathbf{Q}(t)\mathbf{R}(t)$ with $\mathbf{Q}(t)$ as an orthogonal and $\mathbf{R}(t)$ as an upper triangular matrix. In the continuous version of the QR-decomposition, $\mathbf{Q}(t)$ and $\mathbf{R}(t)$ are the unique solutions of

$$\dot{\mathbf{R}}(t) = \mathbf{B}(t)\mathbf{R}(t),\ \mathbf{B}(t) = \mathbf{Q}^\mathsf{T}(t)\mathbf{A}(t)\mathbf{Q}(t) - \mathbf{S}(t) \quad (14)$$

$$\dot{\mathbf{Q}}(t) = \mathbf{Q}(t)\mathbf{S}(t), \quad (15)$$

with $\mathbf{X}(0) = \mathbf{X}_0 = \mathbf{Q}(0)\mathbf{R}(0)$ as some ordered normal Lyapunov basis. The entries s_{ij} of $\mathbf{S} \in \mathbb{R}^{n \times n}$ are given by

$$s_{ij}(t) = \begin{cases} -\mathbf{q}_i^\mathsf{T}(t)\mathbf{A}(t)\mathbf{q}_j(t) & i < j, \\ 0 & i = j, \\ \mathbf{q}_i^\mathsf{T}(t)\mathbf{A}(t)\mathbf{q}_j(t) & i > j, \end{cases} \quad (16)$$

with $\mathbf{q}_i(t)$ as the i-th column of $\mathbf{Q}(t)$. Note that the differential equation (14) is related to the fundamental differential equation (7) via a (stability preserving) Lyapunov

[1] Note that the inequality presented in the original theorem of Barreira and Pesin (2002) is incorrect. This was corrected in an errata.

transformation $\mathbf{R}(t) = \mathbf{Q}^\mathsf{T}\mathbf{X}(t)$, and hence the Lyapunov exponents of (7) and (14) coincide for $\mathbf{X}_0$ as ordered normal Lyapunov basis, see Adrianova (1995). Forward regularity allows to approximate the Lyapunov exponents without explicitly computing the (possibly diverging) solution $\mathbf{X}(t)$ or $\mathbf{R}(t)$.

Definition 2. (Forward regularity). The Lyapunov exponent λ_i^s is called forward regular, if

$$\limsup_{t\to\infty} \frac{1}{t}\int_0^t b_{ii}(s)\mathrm{d}s = \liminf_{t\to\infty} \frac{1}{t}\int_0^t b_{ii}(s)\mathrm{d}s \tag{17}$$

holds with $b_{ii}(t)$ as the corresponding main diagonal element of $\mathbf{B}(t)$. System (5) is called forward regular if all Lyapunov exponents are forward regular.

If the system is forward regular, then, for any ordered normal Lyapunov basis $\mathbf{V} = [\mathbf{v}_1\ \mathbf{v}_2\ \dots\ \mathbf{v}_n]$ of $\mathbb{R}^n$,

$$\begin{aligned}\chi(\mathbf{\Phi}(t,0)\mathbf{v}_i) = \lambda_i^s &= \lim_{t\to\infty}\frac{1}{t}\int_0^t b_{ii}(s)\mathrm{d}s \\ &= \lim_{t\to\infty}\frac{1}{t}\int_0^t \mathbf{q}_i^\mathsf{T}(s)\mathbf{A}(s)\mathbf{q}_i(s)\mathrm{d}s,\end{aligned} \tag{18}$$

see Barreira and Pesin (2002); Tranninger et al. (2020). Hence, the Lyapunov exponents can be approximated by only computing the solution for the orthogonal matrix $\mathbf{Q}(t)$ and evaluating the time average of the diagonal elements $b_{ii} = \mathbf{q}_i^\mathsf{T}\mathbf{A}\mathbf{q}_i$ on a sufficiently large time interval. Typically, only Lyapunov exponents corresponding to unstable or slowly converging modes are of interest. They can be obtained via the reduced QR-decomposition by only considering the first $k \leq n$ columns of $\mathbf{X} = \mathbf{QR}$ according to

$$\dot{\mathbf{R}}_1 = \mathbf{B}_1\mathbf{R}_1,\ \mathbf{R}_1(0) = \mathbf{R}_{1,0} \in \mathbb{R}^{k\times k} \tag{19}$$

$$\mathbf{B}_1 = \bar{\mathbf{Q}}^\mathsf{T}\mathbf{A}\bar{\mathbf{Q}} - \mathbf{S}_1 \tag{20}$$

$$\dot{\bar{\mathbf{Q}}} = \left(\mathbf{I} - \bar{\mathbf{Q}}\bar{\mathbf{Q}}^\mathsf{T}\right)\mathbf{A}\bar{\mathbf{Q}} + \bar{\mathbf{Q}}\mathbf{S}_1,\ \bar{\mathbf{Q}}(0) = \bar{\mathbf{Q}}_0 \in \mathbb{R}^{n\times k}. \tag{21}$$

The matrix $\bar{\mathbf{Q}}$ corresponds to the first k columns of $\mathbf{Q}$ in (15) and hence the elements s_{ij} of $\mathbf{S}_1$ are given according to (16) with $i, j \leq k$. To approximate the k largest Lyapunov exponents, one thus has to solve (21) numerically, compute the diagonal of $\mathbf{B}_1$ and approximate the time average of the diagonal elements on a finite time horizon. Moreover, the columns of $\bar{\mathbf{Q}}$ span an orthogonal complement of the subspace $\mathcal{V}_{k+1}(t)$, i.e. $\mathcal{V}_{k+1}^\perp(t)$, as discussed in Tranninger et al. (2020).

4. EXTENDED SUBSPACE OBSERVER DESIGN

In this section, the subspace observer for LTV systems presented in Tranninger et al. (2020) is recapitulated. Moreover, the (continuous-time) extended Kalman-Bucy filter as an observer for non-linear systems is briefly discussed. Both ideas are combined for the extended subspace observer design in the last part of this section in order to obtain a computationally efficient observer for a class of nonlinear systems.

4.1 Subspace Observer for LTV Systems

The idea for the observer design is to compute the feedback gain only for the subspace $\mathcal{V}_{k+1}^\perp(t)$, which, loosely speaking, can be interpreted as the unstable or slowly converging part of the system. Let the LTV system

$$\dot{\mathbf{x}}(t) = \mathbf{A}(t)\mathbf{x}(t) + \mathbf{B}(t)\mathbf{u}(t) \tag{22a}$$

$$\mathbf{y}(t) = \mathbf{C}(t)\mathbf{x}(t) \tag{22b}$$

be defined on the time interval $\mathbb{J} = [0, \infty)$ with the state $\mathbf{x}(t) \in \mathbb{R}^n$, the input $\mathbf{u}(t) \in \mathbb{R}^m$ and the output $\mathbf{y}(t) \in \mathbb{R}^p$. It is assumed that the matrices $\mathbf{A}(t)$, $\mathbf{B}(t)$ and $\mathbf{C}(t)$ of appropriate dimension are continuous and uniformly bounded . It is furthermore assumed that the autonomous system $\dot{\mathbf{x}}(t) = \mathbf{A}(t)\mathbf{x}(t)$ is forward regular and that the pair $(\mathbf{A}(t), \mathbf{C}(t))$ is uniformly completely observable.

Definition 3. (Uniform Complete Observability). The pair $(\mathbf{A}(t), \mathbf{C}(t))$ is uniformly completely observable if there exist constants β_1, β_2, $T > 0$ such that for all $t_0 \in \mathbb{J}$ it holds that

$$\beta_1\mathbf{I} \preceq \mathbf{M}(t_0 + T, t_0) \preceq \beta_2\mathbf{I} \tag{23}$$

with the observability Gramian

$$\mathbf{M}(t, t_0) = \int_{t_0}^t \mathbf{\Phi}^\mathsf{T}(\tau, t_0)\mathbf{C}^\mathsf{T}(\tau)\mathbf{C}(\tau)\mathbf{\Phi}(\tau, t_0)\mathrm{d}\tau. \tag{24}$$

Uniform complete observability is a standard assumption in Kalman filtering in order to guarantee a uniformly bounded solution of the corresponding filter Riccati equation

$$\dot{\mathbf{P}}_f = \mathbf{A}\mathbf{P}_f + \mathbf{P}_f\mathbf{A}^\mathsf{T} - \mathbf{P}_f\mathbf{C}^\mathsf{T}\mathbf{C}\mathbf{P}_f + \mathbf{G}_f \tag{25}$$

with $\mathbf{G}_f \succ 0$ and $\mathbf{P}_f(t_0) = \mathbf{P}_{f,0} \succ 0$, see Bucy (1972). The observer proposed in Tranninger et al. (2020) can be summarized as follows. Assume that $k^* \leq n$ is the number of non-negative Lyapunov exponents of $\dot{\mathbf{x}} = \mathbf{A}(t)\mathbf{x}$. Then, for any $k \geq k^*$ the proposed observer reads as

$$\dot{\hat{\mathbf{x}}} = \mathbf{A}\hat{\mathbf{x}} + \mathbf{B}\mathbf{u} + \bar{\mathbf{Q}}\mathbf{P}\bar{\mathbf{Q}}^\mathsf{T}\mathbf{C}^\mathsf{T}(\mathbf{y} - \mathbf{C}\hat{\mathbf{x}}),\ \hat{\mathbf{x}}(t_0) = \hat{\mathbf{x}}_0, \tag{26a}$$

$$\dot{\bar{\mathbf{Q}}} = \left(\mathbf{I} - \bar{\mathbf{Q}}\bar{\mathbf{Q}}^\mathsf{T}\right)\mathbf{A}\bar{\mathbf{Q}} + \bar{\mathbf{Q}}\mathbf{S}_1,\ \bar{\mathbf{Q}}(t_0) = \bar{\mathbf{Q}}_0 \tag{26b}$$

$$\dot{\mathbf{P}} = \mathbf{B}_1\mathbf{P} + \mathbf{P}\mathbf{B}_1^\mathsf{T} - \mathbf{P}\bar{\mathbf{Q}}^\mathsf{T}\mathbf{C}^\mathsf{T}\mathbf{C}\bar{\mathbf{Q}}^\mathsf{T}\mathbf{P} + \mathbf{G},\ \mathbf{P}(t_0) = \mathbf{P}_0 \tag{26c}$$

with

$$\mathbf{B}_1 = \bar{\mathbf{Q}}^\mathsf{T}\mathbf{A}\bar{\mathbf{Q}} - \mathbf{S}_1 \in \mathbb{R}^{k\times k} \tag{26d}$$

and a skew-symmetric $\mathbf{S}_1 = -\mathbf{S}_1^\mathsf{T}$ with elements s_{ij} according to (16). It is shown in Tranninger et al. (2020) that with this choice of the observer gain, the estimation error $\mathbf{e}(t) = \mathbf{x}(t) - \hat{\mathbf{x}}(t)$ converges to zero exponentially fast, i.e., the estimation error dynamics

$$\dot{\mathbf{e}}(t) = \left[\mathbf{A}(t) - \bar{\mathbf{Q}}(t)\mathbf{P}(t)\bar{\mathbf{Q}}^\mathsf{T}(t)\mathbf{C}^\mathsf{T}(t)\mathbf{C}(t)\right]\mathbf{e}(t) \tag{27}$$

is exponentially stable.

The matrices $\bar{\mathbf{Q}}$ and $\mathbf{P}$ have dimensions $n \times k$ and $k \times k$, respectively. Note that (26c) is a Riccati equation on a reduced k-dimensional subspace with $\mathbf{P}_0 \succ 0$ and $\mathbf{G} \succ 0$ considered as tuning parameters. The initial condition condition $\bar{\mathbf{Q}}_0$ is chosen as a random orthogonal matrix, see Tranninger et al. (2020). It is crucial to maintain orthogonality of $\bar{\mathbf{Q}}$. Hence, for solving (26b) numerically, a so-called projected integrator as introduced in Dieci et al. (1994) is employed. This is a standard numerical integration scheme combined with a modified Gram-Schmidt algorithm to preserve the orthogonality of $\bar{\mathbf{Q}}$.

4.2 Extended Kalman-Bucy Filter

For a nonlinear system of the form

$$\dot{\mathbf{x}} = \mathbf{f}(\mathbf{x}, \mathbf{u}),\ \mathbf{x}(t_0) = \mathbf{x}_0 \in \mathbb{R}^n \tag{28}$$

with a linear time-varying measurement

$$\mathbf{y} = \mathbf{C}(t)\mathbf{x},\ \mathbf{y}(t) \in \mathbb{R}^p \tag{29}$$

the considered version of the Extended Kalman-Bucy Filter (EKBF) reads as

$$\dot{\hat{\mathbf{x}}} = \mathbf{f}(\hat{\mathbf{x}}, \mathbf{u}) + \mathbf{P}\mathbf{C}^\mathsf{T}(\mathbf{y} - \mathbf{C}\hat{\mathbf{x}}),\ \hat{\mathbf{x}}(t_0) = \hat{\mathbf{x}}_0 \tag{30}$$

$$\dot{\mathbf{P}} = \mathrm{D}\mathbf{f}(\hat{\mathbf{x}}, \mathbf{u})\mathbf{P} + \mathbf{P}\mathrm{D}\mathbf{f}(\hat{\mathbf{x}}, \mathbf{u})^\mathsf{T} - \mathbf{P}\mathbf{C}^\mathsf{T}\mathbf{C}\mathbf{P} + \mathbf{G}, \tag{31}$$

with the matrices $\mathbf{G} \succ 0$ and $\mathbf{P}(t_0)$ of dimension $n \times n$ considered as tuning parameters like, e.g., in Krener (2003). The matrix $\mathrm{D}\mathbf{f}(\hat{\mathbf{x}}, \mathbf{u})$ is the Jacobian of $\mathbf{f}$ evaluated at $\hat{\mathbf{x}}$ and $\mathbf{u}$. Details on the EKBF can be found in (Simon, 2006, Ch. 13.2). Note that in general, only local convergence of the EKBF can be guaranteed, see Krener (2003) for a convergence analysis. To guarantee boundedness of the solution of the corresponding Riccati differential equation, uniform complete observability of $(D\mathbf{f}(\hat{\mathbf{x}}, \mathbf{u}), \mathbf{C})$ is typically required, which is hard to verify in practice. Sufficient conditions for uniform observability are discussed in Krener (2003), but they are still hard to check for practical large order problems.

4.3 Extended Subspace Observer Algorithm

Combining the ideas of the subspace observer for LTV systems and the EKBF from the previous sections allows to propose the extended subspace observer (ESO). The basic idea is to apply the subspace observer to the linear time varying system obtained via the linearization along the estimated trajectory. It is assumed that k^* is the number of non-negative Lyapunov exponents of all trajectories of system (28). For some $k \geq k^*$, the extended subspace observer (ESO) for the nonlinear system (28) with output (29) is then proposed according to

$$\dot{\hat{\mathbf{x}}} = \mathbf{f}(\hat{\mathbf{x}}, \mathbf{u}) + \bar{\mathbf{Q}}\mathbf{P}\bar{\mathbf{Q}}^\mathsf{T}\mathbf{C}^\mathsf{T}(\mathbf{y} - \mathbf{C}\hat{\mathbf{x}}),\ \hat{\mathbf{x}}(t_0) = \hat{\mathbf{x}}_0 \tag{32}$$

and the matrices $\bar{\mathbf{Q}}(t)$ and $\mathbf{P}(t)$ as in (26b) and (26c), respectively, where $\mathbf{A}(t)$ is replaced by $\mathrm{D}\mathbf{f}(\hat{\mathbf{x}}, \mathbf{u})$. The choice of the initial conditions is already discussed in Section 4.1. As a consequence, the dimension of the Riccati differential equation can be drastically reduced if k is small compared to the system order n.

It should be remarked that regularity of the nonlinear system guarantees that the Lyapunov exponents are independent of the specific trajectory, see Frank and Zhuk (2018). Hence, the number of non-negative Lyapunov exponents k^* can be estimated in an off-line simulation.

5. TEMPERATURE PROFILE ESTIMATION AND EXPERIMENTAL RESULTS

Simulation studies showed that system (1) possesses only negative Lyapunov exponents. This allows to implement a trivial observer (TO) without measurement injection.However, the performance of this observer is not satisfying because the convergence behavior cannot be influenced. Moreover, it does not yield an estimate for the total emissivity. The observers presented in Section 4 are thus implemented for the nonlinear model (3). Due to the structure, this model possesses a Lyapunov exponent at zero, which has to be modified in the observer error dynamics. In the following, the extended subspace observer in various configurations is compared with the EKBF. All

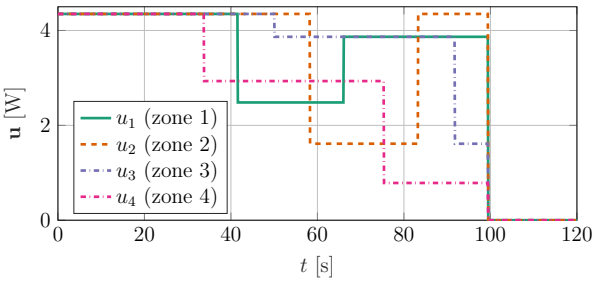

Fig. 2. Electrical power (input) for the four heating zones.

algorithms are implemented in MATLAB/SIMULINK with the fixed step-size solver `ode2 (Heun)` and a step-size of $T_s = 0.1$ s. The ESO is implemented for $k = 6$, $k = 3$ and $k = 1$. The tuning parameters are parametrized via scalars according to $\mathbf{G} = g\mathbf{I}$ and $\mathbf{P}(t_0) = p_0\mathbf{I}$ and identity matrices of appropriate dimensions. For the EKBF and the ESO with $k = 3$ and $k = 6$, the parameters are chosen as $g = 10^{-3}$ and $p_0 = 1$; for the ESO with $k = 1$, $p_0 = 1$ and $g = 1$ was chosen to obtain a similar convergence speed as for the other observers.

The experiments are conducted with a pseudo-random electrical heat power input as depicted in Fig. 2. The obtained measurements are fed offline into the SIMULINK model with the implemented observer algorithms. In Fig. 3 the temperature estimates in the four heating zones for the different observers are compared with the measurements of the pyrometers. Note that below 300 °C, the pyrometers do not provide reliable measurements due to their measurement principle. One can see that the temperature estimates are qualitatively comparable for all implemented observers. The emissivity estimates are depicted in Fig. 4. The estimates are reasonable because the experiment was carried out with a highly doped wafer with an emissivity of approximately 0.85.

Remarkably, the ESO for $k = 1$ requires to solve a scalar Riccati differential equation only but still delivers reasonable temperature and emissivity estimates. In contrast to the extended Kalman-Bucy filter, which requires to solve a differential equation of order $n+(\frac{n^2-n}{2}+n) = \frac{1}{2}n^2+\frac{3}{2}n$, the proposed ESO requires to solve a differential equation of order $n+nk+\left(k + \frac{k^2-k}{2}\right) = n+k(n+1+\frac{k-1}{2})$. For the ESO with $k = 1$, this reduces to a differential equation of order 61 compared to 495 for the EKBF. The whole temperature profile estimate for the ESO with $k = 1$ is depicted in Fig. 5 together with all pyrometer measurements. This also shows the satisfying performance of the proposed observer design technique.

6. DISCUSSION AND OUTLOOK

This paper presents a computationally efficient observer concept for the temperature profile estimation of silicon wafers. The observer feedback gain is computed via a reduced order Riccati differential equation. The proposed observer is compared to a classical extended Kalman-Bucy filter and shows comparable performance at a drastically reduced computational cost. A future research direction is the investigation of convergence conditions for the proposed observer for general nonlinear estimation problems.

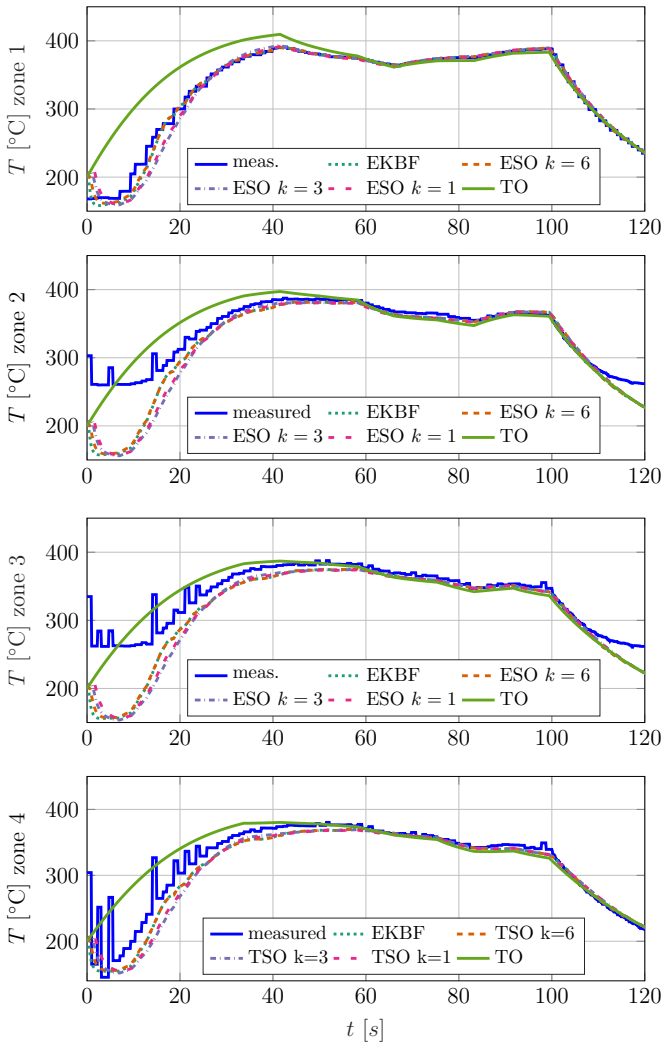

Fig. 3. Comparison of estimates and measurements in the four zones.

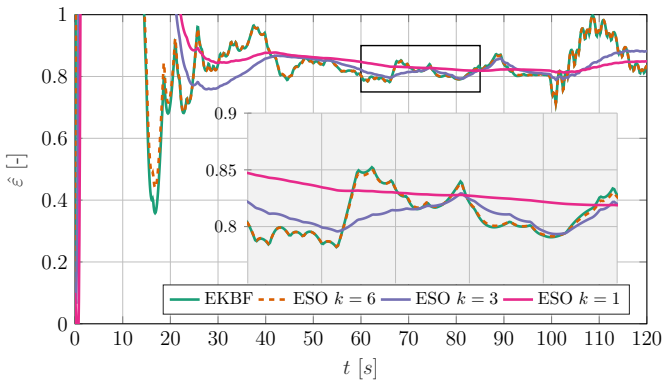

Fig. 4. Comparison of emissivity estimates for different observers.

Also the comparison of different solvers and discrete time implementations may be subject of future research.

REFERENCES

Adrianova, L.Y. (1995). *Introduction to Linear Systems of Differential Equations (Translations of Mathematical Monographs)*. American Mathematical Society.

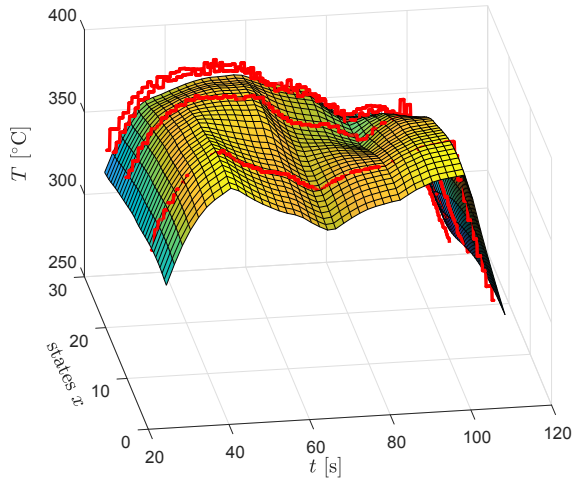

Fig. 5. ESO estimation results together with the pyrometer measurements for $k = 1$.

Ali, J.M., Hoang, N.H., Hussain, M., and Dochain, D. (2015). Review and classification of recent observers applied in chemical process systems. *Computers & Chemical Engineering*, 76, 27–41. doi: 10.1016/j.compchemeng.2015.01.019.

Barreira, L. and Pesin, Y.B. (2002). *Lyapunov Exponents and Smooth Ergodic Theory (University Lecture Series)*. Amer Mathematical Society.

Bucy, R.S. (1972). The riccati equation and its bounds. *Journal of Computer and System Sciences*, 6(4), 343–353. doi:10.1016/s0022-0000(72)80026-6.

Dieci, L., Russell, R.D., and Vleck, E.S.V. (1994). Unitary integrators and applications to continuous orthonormalization techniques. *SIAM Journal on Numerical Analysis*, 31(1), 261–281. doi:10.1137/0731014.

Dieci, L. and Van Vleck, E.S. (2007). Lyapunov and sacker–sell spectral intervals. *Journal of Dynamics and Differential Equations*, 19(2), 265–293. doi: 10.1007/s10884-006-9030-5.

Frank, J. and Zhuk, S. (2018). A detectability criterion and data assimilation for nonlinear differential equations. *Nonlinearity*, 31(11), 5235–5257. doi:10.1088/1361-6544/aaddcb.

Kleindienst, M., Reichhartinger, M., Horn, M., and Staudegger, F. (2018). Observer-based temperature control of an LED heated silicon wafer. *Journal of Process Control*, 70, 96–108. doi:10.1016/j.jprocont.2018.07.006.

Kleindienst, M., Reichhartinger, M., Koch, S., and Horn, M. (2019). A distributed-parameter approach for the surface temperature estimation of an LED heated silicon wafer. *IEEE Transactions on Semiconductor Manufacturing*, 1–1. doi:10.1109/tsm.2019.2931979.

Krener, A.J. (2003). The convergence of the extended kalman filter. In *Directions in Mathematical Systems and Theory*.

Simon, D. (2006). *Optimal State Estimation*. John Wiley & Sons Inc.

Tranninger, M., Seeber, R., Zhuk, S., Steinberger, M., and Horn, M. (2020). Detectability analysis and observer design for linear time varying systems. *IEEE Control Systems Letters*, 4(2), 331–336. doi: 10.1109/lcsys.2019.2927549.